Polymer Journal, Vol. 39, No. 8, pp. 783–791 (2007)

Characterization of Wormlike Pentaoxyethylene Dodecyl Ether $C_{12}E_5$ Micelles Containing *n*-Dodecanol

Maiko MIYAKE and Yoshiyuki EINAGA†

Department of Chemistry, Nara Women's University, Kitauoyanishi-machi, Nara 630-8506, Japan

(Received March 28, 2007; Accepted May 2, 2007; Published June 19, 2007)

ABSTRACT: Variation of characteristics of the wormlike micelles formed with the surfactant pentaoxyethylene dodecyl ether $C_{12}E_5$ with uptake of *n*-dodecanol were examined by static (SLS) and dynamic light scattering (DLS) experiments. The SLS results have been analyzed with the aid of the light scattering theory for micelle solutions to yield the molar mass $M_w(c)$ as a function of concentration c along with the cross-sectional diameter d of the micelle. The apparent hydrodynamic radius $R_{H,app}(c)$ determined by DLS as a function of c is also successfully analyzed by a fuzzy cylinder theory which takes into account the hydrodynamic and direct collision interactions among micelles, allowing us to evaluate the stiffness parameter λ^{-1}. It has been found that the micellar length increases with increasing concentration c or with raising temperature T irrespective of the composition of the $C_{12}E_5$ + *n*-dodecanol system. The length of the micelles at fixed c and T steeply increases with increasing weight fraction w_d of *n*-dodecanol. The values of d and λ^{-1} are found to increase with increasing w_d. On the other hand, the spacing s between the hydrophilic tails of adjacent surfactant molecules on the micellar surface decreased with w_d. It has been shown for the $C_{12}E_5$, $C_{10}E_5$, and $C_{12}E_6$ that the values d, s, and λ^{-1} are substantially independent of the hydrophobic and hydrophilic chain length of the surfactant molecules. [doi:10.1295/polymj.PJ2006276]

KEY WORDS Wormlike Micelle / Light Scattering / Phase Diagram / Radius of Gyration / Diffusion Coefficient / Hydrodynamic Radius / Polyoxyethylene Alkyl Ether / Surfactant /

For the micelles of nonionic surfactant polyoxyethylene alkyl ethers $H(CH_2)_i(OCH_2CH_2)_jOH$ (abbreviated C_iE_j) and their binary mixtures, we have investigated micellar characteristics such as the weight-average molar mass M_w, mean-square radius of gyration $\langle S^2 \rangle$, hydrodynamic radius R_H, and intrinsic viscosity $[\eta]$ as functions of surfactant mass concentration c by static (SLS) and dynamic light scattering (DLS) measurements and viscometry.[1–9] In these work, we were able to determine the concentration-dependent characteristics of the micelles unequivocally by separating the contributions of the thermodynamic and hydrodynamic interactions to the SLS and DLS results with the aid of the corresponding theories. We have determined the values of $M_w(c)$ at a specified c along with the cross-sectional diameter d of the micelles from the analysis of the SLS data by using a molecular thermodynamic theory[10,11] formulated with the wormlike spherocylinder model. The molar mass M_w dependence of $\langle S^2 \rangle$, R_H, and $[\eta]$ is quantitatively represented by the chain statistical[12] and hydrodynamic[13–16] theories based on the wormlike chain and spherocylinder models, respectively, thereby yielding the values of the stiffness parameter λ^{-1}. The salient features found for the C_iE_j micelles are summarized as: (i) The micelles grow in length to a greater extent for larger i and smaller j. (ii) The d values do not significantly vary with the values of i and j. (iii) The stiffness parameter λ^{-1} decreases with increasing i at fixed j and increases with increasing j at fixed i.

We have also studied $C_{10}E_5$ and $C_{12}E_6$ micelles containing *n*-dodecanol to explore effects of uptake *n*-alcohol into the micelles on the micellar characteristics.[17,18] It has been then found that the SLS and DLS results are successfully analyzed in a similar fashion to the micelle solutions of single C_iE_j or their binary mixtures. In particular, it has been demonstrated that the fuzzy cylinder theory[19–21] is applied in a favorable way to analyze the apparent hydrodynamic radius $R_{H,app}$, thereby obtaining the concentration-dependent micellar growth by separating contributions of the enhancement of hydrodynamic interactions among micelles with c. From the analyses, we have found that the micelles are well described with the wormlike spherocylinder model and that the micellar length L, cross-sectional diameter d, and stiffness parameter λ^{-1} increase with *n*-dodecanol content in the micelles.

In the present study, we extend the studies to micelles of the $C_{12}E_5$ + *n*-dodecanol + water system to investigate effects of hydrophobic i and hydrophilic chain lengths j. The results are, thus, compared with those of the $C_{10}E_5$ and $C_{12}E_6$ micelles containing *n*-dodecanol. The $C_{12}E_5$ micelles containing an oil such as *n*-octane, *n*-decane, *n*-dodecane, phospholipid, and so forth were extensively studied by SLS, DLS, small-

†To whom correspondence should be addressed (E-mail: einaga@cc.nara-wu.ac.jp).

angle neutron scattering, and other methods.[22–32] In the range of small oil content, $C_{12}E_5$ is found to form wormlike micelles at low concentrations of the surfactant + oil in the L_1 phase. These authors, however, almost exclusively deal with apparent quantities such as apparent molar mass M_{app} and apparent hydrodynamic radius $R_{H,app}$ and then characteristics of the micelles in an "isolated" state is not determined unequivocally. In this work, we follow the technique mentioned above to characterize "isolated" micelles at finite c by evaluating separately the thermodynamic and hydrodynamic interactions among micelles.

EXPERIMENTAL SECTION

Materials

The surfactant $C_{12}E_5$ sample and *n*-dodecanol were purchased from Nikko Chemicals Co. Ltd. and Nakaraitesque Co., respectively, and used without further purification. The solvent water used was high purity (ultrapure) water prepared with Simpli Lab water purification system of Millipore Co.

Phase Diagram

Cloud-point temperature of a given micelle solution was determined as the temperature at which the intensity of the laser light transmitted through the solution abruptly decreased when temperature was gradually raised.

$C_{12}E_5$ micelle solutions were prepared by dissolving $C_{12}E_5$ in water with adding appropriate amount of *n*-dodecanol with a microliter syringe (Hamilton). Complete mixing and micelle formation were achieved by stirring the solutions using a magnetic stirrer for at least one day. *n*-Dodecanol is substantially insoluble in water and thus completely incorporated into the micelles. The weight fractions w of micelle solutions were determined gravimetrically and converted to mass concentrations c by the densities ρ of the solutions given below. Throughout this paper, w and c denote the weight fraction and mass concentration of $C_{12}E_5$ + *n*-dodecanol in the $C_{12}E_5$ + water + *n*-dodecanol ternary solutions. *n*-Dodecanol content in the $C_{12}E_5$ + *n*-dodecanol mixture is represented by its weight fraction w_d.

Static Light Scattering

The scattering intensities were measured for micelle solutions of various w_d at 15.0 °C and for those of $w_d = 0.0150$ at 15.0 and 20.0 °C. The ratio $Kc/\Delta R_\theta$ was obtained for each solution as a function of the scattering angle θ ranging from 30 to 150° and extrapolated to zero scattering angle to evaluate $Kc/\Delta R_0$. Here, c is the mass concentration of surfactant + *n*-dodecanol, ΔR_θ is the excess Rayleigh ratio, and K is the optical constant defined as

$$K = \frac{4\pi^2 n^2 (\partial n/\partial c)_{T,p}^2}{N_A \lambda_0^4} \tag{1}$$

with N_A being the Avogadro's number, λ_0 the wavelength of the incident light in vacuum, n the refractive index of the solution, $(\partial n/\partial c)_{T,p}$ the refractive index increment, T the absolute temperature, and p the pressure. The plot of $Kc/\Delta R_\theta$ *vs.* $\sin^2(\theta/2)$ affords a good straight line for all the micelle solutions studied.

The apparatus used is an ALV DLS/SLS-5000/E light scattering photogoniometer and correlator system with vertically polarized incident light of 632.8 nm wavelength from a Uniphase Model 1145P He-Ne gas laser.

The micellar solutions were prepared in the same way as those for the cloud-point measurements described above. The experimental procedure is the same as described before.[1–5,7–9,18] In the present study, we have treated the micelle solutions as the binary system which consists of micelles containing *n*-dodecanol as a solute and water as a solvent.

The results for the refractive index increment $(\partial n/\partial c)_{T,p}$ measured at 632.8 nm with a Union Giken R601 differential refractometer are summarized as (in cm^3/g):
For 10.0 °C ≤ T ≤ 25.0 °C,

$$(\partial n/\partial c)_{T,p} = 0.137 - 3.18 \times 10^{-4}(T - 273.15) \quad (w_d = 0.0150) \tag{2}$$

$$(\partial n/\partial c)_{T,p} = 0.138 - 3.20 \times 10^{-4}(T - 273.15) \quad (w_d = 0.0299) \tag{3}$$

$$(\partial n/\partial c)_{T,p} = 0.138 - 3.65 \times 10^{-4}(T - 273.15) \quad (w_d = 0.0499) \tag{4}$$

Dynamic Light Scattering

DLS measurements were carried out to determine the translational diffusion coefficient D for the micelles by the use of the same apparatus and light source as used in the SLS studies described above. All the test solutions studied are the same as those used in the SLS studies. From the D values obtained by the cumulant method for the normalized autocorrelation function $g^{(2)}(t)$, the apparent hydrodynamic radius $R_{H,app}$ has been evaluated by the defining equation[18,33–35]

$$D = \frac{(1 - vc)^2 M_w k_B T}{6\pi\eta_0 R_{H.app}} \left(\frac{Kc}{\Delta R_0}\right) \tag{5}$$

where v is the partial specific volume of the solute

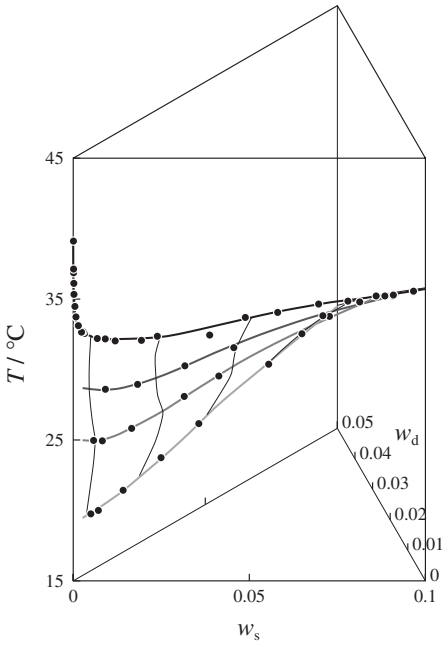

Figure 1. Three-dimensional representation of the binodal surface for the $C_{12}E_5$ + *n*-dodecanol + water system: w_s, weight fraction of $C_{12}E_5$ in the solution; w_d, weight fraction of *n*-dodecanol in the $C_{12}E_5$ + *n*-dodecanol mixture. The data points for $w_d = 0$ are the literature results of Ref 5.

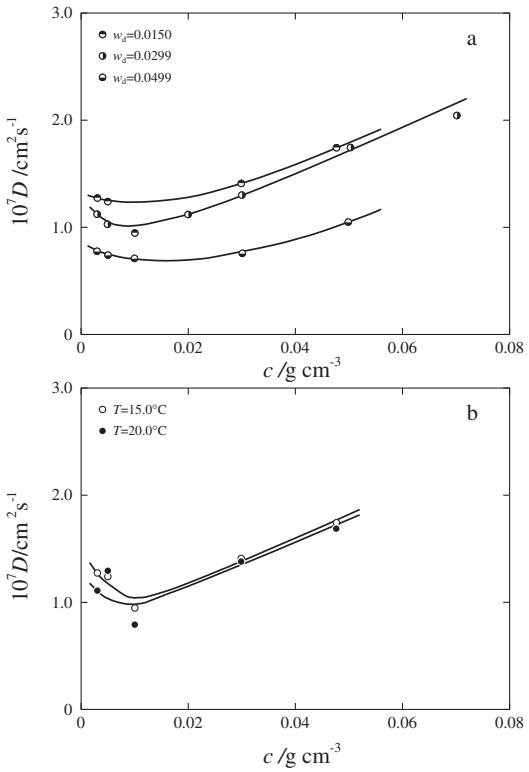

Figure 2. Concentration dependence of mutual diffusion coefficient D for the $C_{12}E_5$ containing *n*-dodecanol for various w_d indicated at $T = 15.0\,^\circ$C (a) and at indicated temperatures for $w_d = 0.0150$ (b).

(micelle), k_B is the Boltzmann constant, and η_0 is the solvent viscosity.

Density

For all the micelle solutions containing *n*-dodecanol, the solution density ρ has been found to be independent of micelle weight fraction w and *n*-dodecanol content w_d at every temperature examined, *i.e.*, from 10.0 to 25.0 °C. Thus we have used the literature values of the density ρ_0 of pure water at corresponding temperatures for ρ, and the values of v of the micelles have been calculated as ρ_0^{-1}.

RESULTS

Phase Behavior

Figure 1 illustrates 3D phase diagrams for the ternary system $C_{12}E_5$ + *n*-dodecanol + water constructed from the cloud point data, along with the literature results at $w_d = 0$.[5] Here, w_s is the weight fraction of the surfactant $C_{12}E_5$ in the solution. We find that the phase boundaries significantly shift to lower temperatures as w_d increases. The temperature shift with w_d is more significant at lower w_s. All the light scattering experiments have been performed in the L_1 phase below the binodal surface.

Mutual Diffusion Coefficient

In Figure 2a and b, the mutual diffusion coefficient D are double-logarithmically plotted against c examined at various w_d at $T = 15.0\,^\circ$C and at 15.0 and 20.0 °C at $w_d = 0.0150$, respectively. The data points at fixed w_d in Figure 2a and at fixed T in Figure 2b follow a curve convex downward. The D value decreases with increasing w_d or T, suggesting that the micelles grow with increasing *n*-dodecanol content w_d or temperature T.

DISCUSSION

Analysis of SLS Data

As mentioned in the Introduction, we have analyzed the present SLS data by employing Sato theory for static light-scattering from micellar solutions[10,11] with wormlike spherocylinder model with the total length L, cross-sectional diameter d, and stiffness λ^{-1} in order to determine M_w of the micelles at a specific concentration c. The expression for $Kc/\Delta R_0$ is written by

$$\frac{Kc}{\Delta R_0} = \frac{1}{M_w(c)} + 2A(c)c \qquad (6)$$

where $M_w(c)$ is the weight-average molar mass of the micelles and $A(c)$ is the apparent second virial coefficient in a sense that it is comprised of the second, third, and the higher virial coefficient terms. $M_w(c)$ and $A(c)$ are functions of c, containing three parameters d, free-energy parameter g_2 which controls micel-

lar growth, and depth $\hat{\epsilon}$ of the attractive potential between spherocylinders. In these, g_2 represents the difference in Gibbs free energy between surfactant molecules located in the end-capped portion and those in the central cylindrical portion of the micelle. Here, we refer details of the functions $M_w(c)$ and $A(c)$ to the original papers (Ref 10 and 11) and our previous papers.[1,3]

As in the case of the previous work,[18] we have treated present micelle solutions as two component systems consisting of micelles and solvent, although they include three components: surfactant $C_{12}E_5$, *n*-dodecanol, and water. It has been assumed in the analyses that the composition of $C_{12}E_5$ + *n*-dodecanol in the micelles is given by w_d. The weight average molecular weight of the $C_{12}E_5$ + *n*-dodecanol mixture calculated with a given w_d was used as the surfactant molecular weight M_0 required in the theoretical analysis.

Figure 3a and b demonstrate the results of curve-fitting of the theoretical calculations to the experimental values of $Kc/\Delta R_0$ for the micelle solutions of various w_d indicated at 15.0 °C (a) and of $w_d = 0.0150$ at 15.0 and 20.0 °C (b), respectively. The solid curves which represent the best-fit theoretical curves well coincide with the respective data points at given w_d or T. The good agreement implies that the micelles containing *n*-dodecanol are well represented by the wormlike spherocylinder model. The dashed lines represent the values of $1/M_w(c)$ at respective w_d or T. For all the micelles at any fixed w_d and T, they are straight lines with a slope of -0.5, showing that M_w increases with c following a relation $M_w \propto c^{1/2}$ in the range of c examined, as in the case of the previous findings for the micelles formed with single surfactant of various type,[1–5,7] for those formed with binary C_iE_j mixtures,[8,9] and the $C_{10}E_5$ micelles containing *n*-dodecanol.[18] These results are in good correspondence with simple theoretical predictions derived from the thermodynamic treatments of multiple equilibria among micelles of various aggregation numbers.[10,36–38] The increase in $M_w(c)$ with increasing c and w_d and with raising temperature is consistent with our previous results for the $C_{10}E_5$ + *n*-dodecanol micelles[18] and the findings by Menge *et al.*[22,23] for the $C_{12}E_5$ + *n*-decane micelles. The solid and dashed curves coincide with each other at small c but the former rapidly increases with increasing c, deviating upward from the latter. The results indicate that contributions of the virial coefficient terms, that is, the second term of the right hand side of eq 6, to $Kc/\Delta R_0$ are negligible at small c but progressively increase with increasing c as expected.

The d value determined by the curve fitting was independent of T but gradually increased with w_d. They

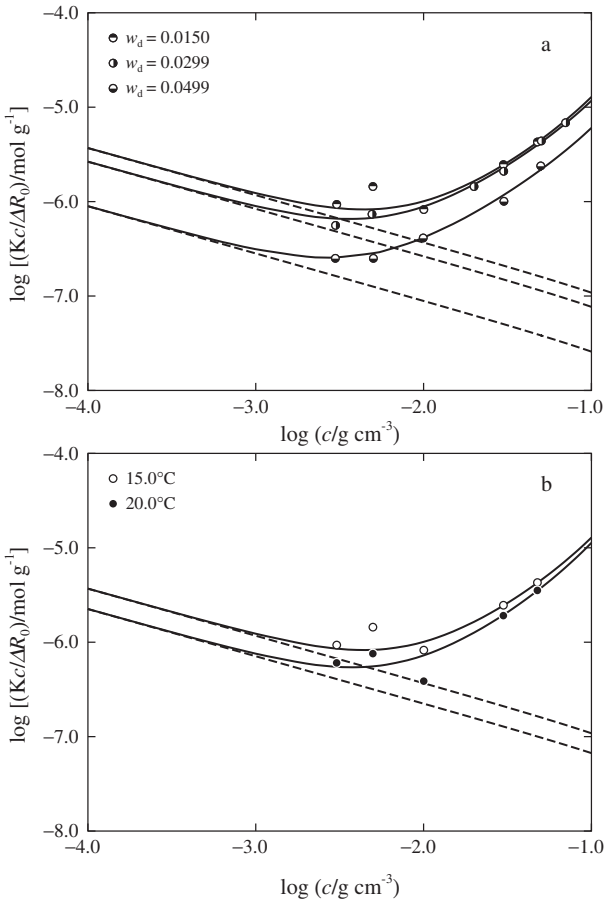

Figure 3. Results of the curve fitting for the double-logarithmic plots of $Kc/\Delta R_0$ against c for the $C_{12}E_5$ + *n*-dodecanol + water system for various w_d indicated at $T = 15.0$ °C (a) and at indicated temperatures for $w_d = 0.0150$ (b): The solid and dashed curves represent the calculated values of $Kc/\Delta R_0$ and $1/M_w(c)$, respectively.

were 3.3, 3.5, and 4.4 nm at $w_d = 0.0150$, 0.0299, and 0.0499, respectively. The present finding is in qualitative agreement with SANS results by Menge *et al.*[24] for $C_{12}E_5$ micelles containing *n*-decane.

Figure 4 shows g_2 and $\hat{\epsilon}$ as functions of w_d for the $C_{12}E_5$ micelles containing *n*-dodecanol at 15.0 °C. We find that g_2 is an increasing function of w_d, corresponding to the results that the micelles grow in molecular weight with increasing w_d as found in Figure 3a. It is seen that $\hat{\epsilon}$ decreases with increasing w_d but its meaning is not clear at present.

Mean-Square Radius of Gyration

On the basis of the fundamental light-scattering equation for dilute polymer solutions

$$\frac{Kc}{\Delta R_\theta} = \left(\frac{1}{M_w} + 2A_2c + \cdots\right) + \left(\frac{\langle S^2\rangle}{3M_w}q^2 + \cdots\right) \quad (7)$$

$$q = \frac{4\pi n}{\lambda_0}\sin(\theta/2) \quad (8)$$

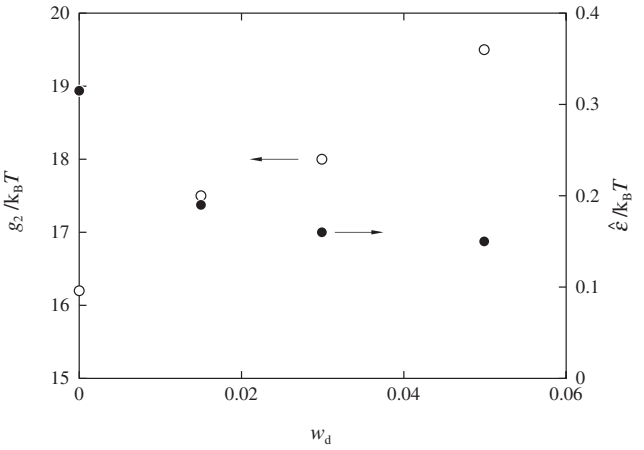

Figure 4. Plots of g_2 (unfilled circles) and $\hat{\epsilon}$ (filled circles) against w_d for the $C_{12}E_5$ micelle solutions containing *n*-dodecanol.

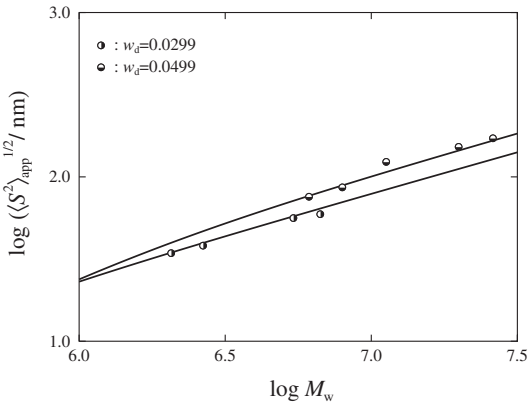

Figure 5. Double-logarithmic plots of root mean-square radius of gyration $\langle S^2\rangle^{1/2}$ against M_w for the $C_{12}E_5$ micelles containing *n*-dodecanol for indicated w_d at $T = 15.0\,^\circ$C: The solid curves represent the calculated values (see the text).

we have determined the apparent mean-square radius of gyration $\langle S^2\rangle_{app}$ for the $C_{12}E_5$ micelles containing *n*-dodecanol at finite c from the slope of the $Kc/\Delta R_\theta$ versus $\sin^2(\theta/2)$ plot. Here, $\langle S^2\rangle$ is the mean-square radius of gyration, A_2 is the second virial coefficient, q is the magnitude of the scattering vector, and λ_0 is the wave length of the incident light in vacuum. It should be noted that for micelle solutions, the former two quantities $\langle S^2\rangle$ and A_2 are concentration-dependent, since the size of the solutes (micelles in this case) varies with concentration c. In the evaluation, we used the M_w values determined as described above at each given c. Since $\langle S^2\rangle$ is possibly affected by intermicellar interactions, it is denoted by $\langle S^2\rangle_{app}$.

Molar mass dependence of $\langle S^2\rangle^{1/2}$ is exhibited in Figure 5 for the $C_{12}E_5$ + *n*-dodecanol micelles with $w_d = 0.0299$ and 0.0499 at 15.0 °C. As shown by the solid curves, the data points for each fixed w_d form a single curve and are quantitatively represented by the theoretical values calculated by Benoit-Doty equation[12]

$$\lambda^2\langle S^2\rangle = \frac{\lambda L}{6} - \frac{1}{4} + \frac{1}{4\lambda L} - \frac{1}{8\lambda^2 L^2}(1 - e^{-2\lambda L}) \quad (9)$$

for wormlike polymers along with the relation

$$L_w = \frac{4\nu M_w}{\pi N_A d^2} + \frac{d}{3} \quad (10)$$

Here, the relation is derived from the micellar volume and L_w is used in place of L in eq 9. In the calculation, the d values obtained from SLS results in the preceding section were used and then the λ^{-1} values were determined as 22 nm at $w_d = 0.0299$ and 60 nm at $w_d = 0.0499$ to achieve the best fit to the experimental results.

Hydrodynamic Radius of the Micelles

Figure 6a and 6b depict bilogarithmic plots of

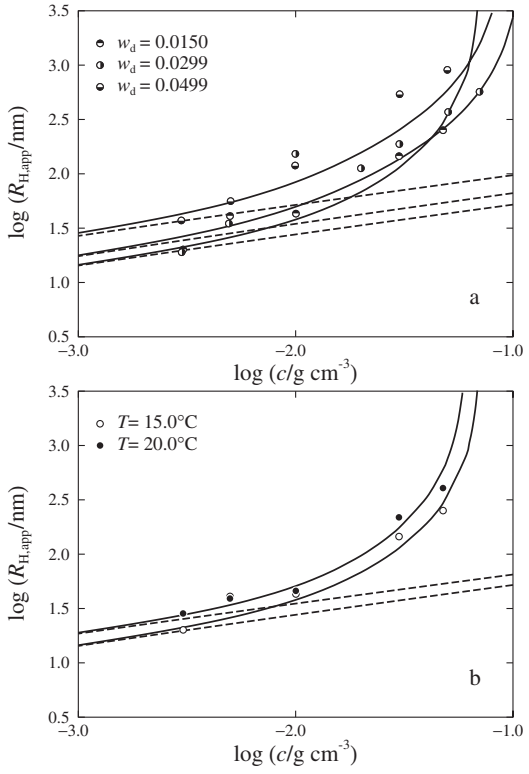

Figure 6. Double-logarithmic plots of the apparent hydrodynamic radius $R_{H,app}$ against c for the $C_{12}E_5$ micelles containing *n*-dodecanol for various w_d indicated at $T = 15.0\,^\circ$C (a) and for $w_d = 0.0150$ at indicated temperatures (b): Solid and dashed curves represent the calculated values with and without the intermicellar hydrodynamic interactions (see the text).

$R_{H,app}$ determined by eq 5 from the D data in Figure 2 against c for the $C_{12}E_5$ + *n*-dodecanol micelles of various w_d at 15.0 °C and of $w_d = 0.0150$ at 15.0 and 20.0 °C, respectively. It is seen that at any given w_d and T, $R_{H,app}$ increases with increasing c. The $R_{H,app}$ values do not, however, necessarily correspond to those for "isolated" micelles. The increase of $R_{H,app}$

reflects both micellar growth in size and enhancement of the effects of the intermicellar hydrodynamic interactions with increasing c. $R_{H,app}$ as a function of c may be represented as

$$R_{H,app}(c) = R_H(c)H(c) \tag{11}$$

where $R_H(c)$ represents the hydrodynamic radius of a "isolated" micelle which may grow in size with c and $H(c)$ the hydrodynamic interactions which may be enhanced with c. In these two functions, $R_H(c)$ may be calculated by employing the equations formulated for the translational friction coefficient by Norisuye *et al.*[13] with wormlike spherocylinder model near the rod limit and by Yamakawa *et al.*[14,15] with the wormlike cylinder model, as a function of the micellar length L with including d and the stiffness parameter λ^{-1}. Their equation for R_H reads

$$R_H = \frac{L}{2f(\lambda L, \lambda d)} \tag{12}$$

The expression for the function f is so lengthy that we refer it to the original papers.[13–15] We are able to calculate $R_H(c)$ required in eq 11, by combining eq 12 with eq 10. Here, L_w by eq 10 is used in place of L in eq 12 and the M_w values as a function of c are obtained from the dashed lines in Figure 3.

The function $H(c)$ in eq 11 may be calculated with the formulation given by Sato *et al.*[19–21] They have recently treated with the concentration dependence of the intermolecular hydrodynamic and direct collision interactions among wormlike polymer chains by using a fuzzy cylinder model. The fuzzy cylinder is defined as a cylinder which encapsulate a wormlike chain or a wormlike spherocylinder in the present case. Its effective length and diameter are evaluated from the wormlike chain parameters L, d, and λ^{-1}. In the formulation, Sato *et al.* have taken into account the hydrodynamic interactions among fuzzy cylinders and also jamming effects of the cylinders on the longitudinal and transverse diffusion coefficients along and perpendicular to the chain end-to-end axis, respectively.

Combining Sato *et al.*'s $H(c)$, eqs 10 and 12 with the experimental results for $M_w(c)$, we have calculated $R_{H,app}(c)$ by eq 11. The solid curves in Figure 6a and b are the theoretical values thus calculated. Here, we have used the d values obtained from the analyses of the SLS data and the values of λ^{-1} determined so as to achieve the best fit to the observed results. The λ^{-1} values obtained are 24, 32, and 34 nm at w_d = 0.0150, 0.0299, and 0.0499, respectively. They were independent of temperature T. As found in Figure 6, the theoretical results are in good coincidence with the observed ones, although the data points are somewhat scattered and discrepancy between observed and calculated results are found in some cases, especially at large w_d in Figure 6a. The dashed lines represent relationships between R_H and c for the isolated micelles without any intermicellar hydrodynamic interaction, and thus the growth of the micelles with increasing c. We find that the difference between the solid and corresponding dashed lines, *i.e.*, $R_{H,app}$ and R_H, becomes progressively large with c, and that a great portion of $R_{H,app}$ results from the hydrodynamic interactions at large c. On the other hand, the increase of the micellar size with c is rather moderate.

In Figure 7, the same observed and theoretical results for $R_{H,app}$ and R_H as those in Figure 6 are shown as functions of M_w in the bilogarithmic plots. Here, the dashed lines correspond to the theoretical values of R_H calculated by eq 12 combined with eq 10. They asymptotically approach the data points and the solid curves as M_w is decreased, *i.e.*, as c is lowered, indicating that the effects of the intermicellar hydrodynamic interactions on $R_{H,app}$ become negligible in the asymptotic region of low c. The results are in line with our previous findings for R_H of the single C_iE_j micelles.[1–3] At any given w_d at fixed T, the difference between the solid and dashed curves, which steeply

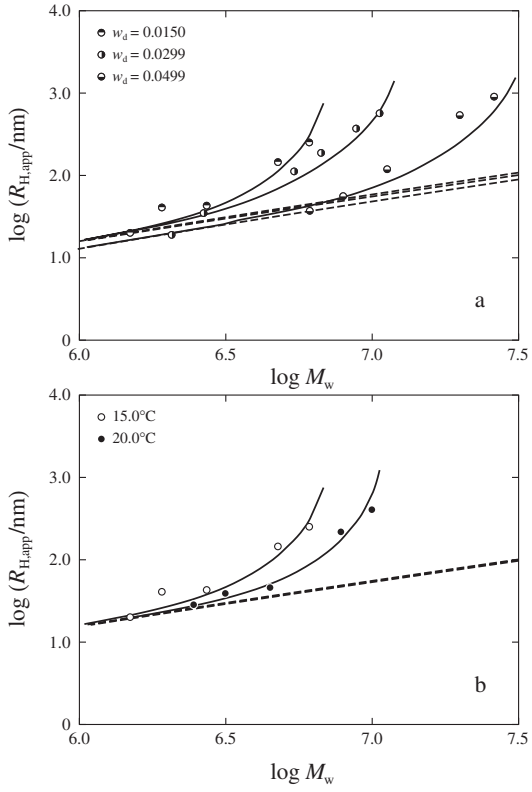

Figure 7. Double-logarithmic plots of the apparent hydrodynamic radius $R_{H,app}$ against W_w for the $C_{12}E_5$ micelles containing *n*-dodecanol for various w_d indicated at T = 15.0 °C (a) and for w_d = 0.0150 at indicated temperatures (b): Solid and dashed curves represent the calculated values with and without the intermicellar hydrodynamic interactions (see the text).

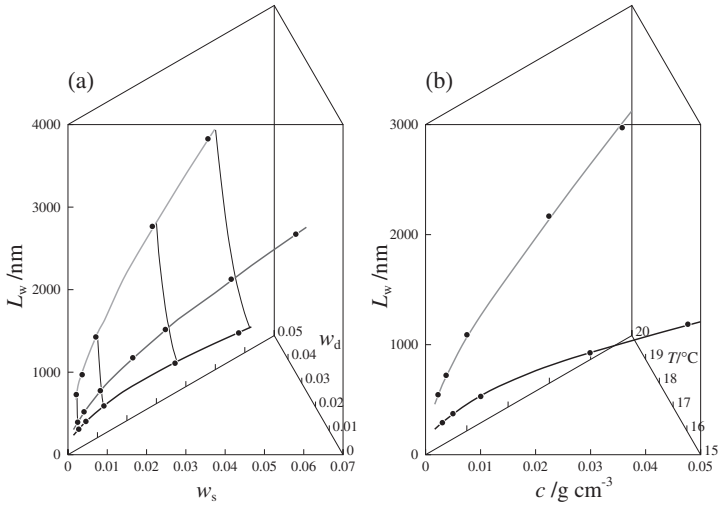

Figure 8. The weight-average micellar length L_w as a function of w_s and w_d at 15.0 °C (a) and as a function of c and T for $w_d = 0.0150$ (b) for the $C_{12}E_5$ + *n*-dodecanol micelles.

increase with M_w, is due to the enhancement of the intermicellar hydrodynamic and dynamic interactions with increasing c, *i.e.*, the contribution of $H(c)$ to $R_{H,app}(c)$ in eq 11.

The Micellar Length

Figure 8a and b depict the weight-average length L_w of the $C_{12}E_5$ micelles containing *n*-dodecanol as a function of the surfactant weight fraction w_s and w_d at $T = 15.0$ °C (a) and as a function of c and T at $w_d = 0.0150$ (b), respectively. Here, L_w has been calculated by eq 10 from the values of $M_w(c)$ and d obtained above from the analyses of the SLS data. It is found that the micelles at a given w_d or T, L_w becomes larger as w_s or c is increased. As seen in these figures, L_w at fixed w_s or c steeply increases with increasing w_d, *i.e.*, with uptake of *n*-dodecanol into the micelles. The results are consistent with the finding by Menge *et al.*[22] for the $C_{12}E_5$ micelles containing *n*-decane.

Figure 8b shows that the length L_w at fixed c significantly increases with raising temperature. This finding is in line with our previous results[1–7] for the micelles of the single surfactant C_iE_j. It is also in qualitative agreement with the results reported by Menge *et al.*[23] for the $C_{12}E_5$ + *n*-decane micelles and those by Kwon and Kim[31] for the $C_{12}E_5$ + phospholipid micelles.

Variation of Characteristics of the $C_{10}E_5$, $C_{12}E_5$, and $C_{12}E_6$ Micelles with uptake of n-Dodecanol

Figure 9 depicts w_d dependence of d for the $C_{12}E_5$ micelles containing *n*-dodecanol along with the previous results[18] for the $C_{10}E_5$ and $C_{12}E_6$ micelles containing *n*-dodecanol. The d values of these micelles increase with increasing *n*-dodecanol content in the micelles. It is found that they are larger for the $C_{12}E_5$ micelles than for the $C_{10}E_5$ and $C_{12}E_6$ micelles. The dependence of the d values on the hydrophobic and hydrophilic chain length is not, however, systematic and thus, we cannot derive definite conclusion about the dependence at present.

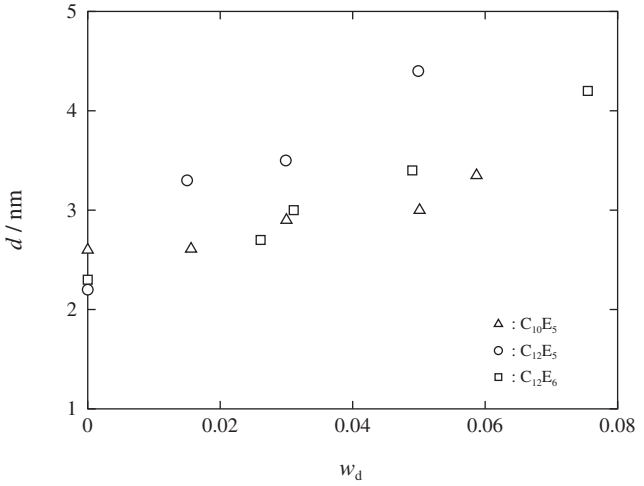

Figure 9. The micellar cross-sectional diameter d as a function of w_d for the $C_{10}E_5$ micelles at 20.0 °C (triangles), $C_{12}E_5$ micelles at 15.0 °C (circles), and $C_{12}E_6$ micelles at 25.0 °C (squares) containing *n*-dodecanol.

The values of the spacing s between the hydrophilic tails of adjacent surfactant molecules on the micellar surface are evaluated from the values of d, L_w, and the aggregation number N_w calculated from M_w. Here, the surface area of the spherocylindrial micelles was calculated from the values of d and L_w, and then dividing it by the aggregation number N_w yielded the values of the area occupaied by each surfactant molecule, from which the spacing s was evaluated. They are plotted against w_d in Figure 10, along with the results for $C_{10}E_5$ and $C_{12}E_6$ micelles. The s value is

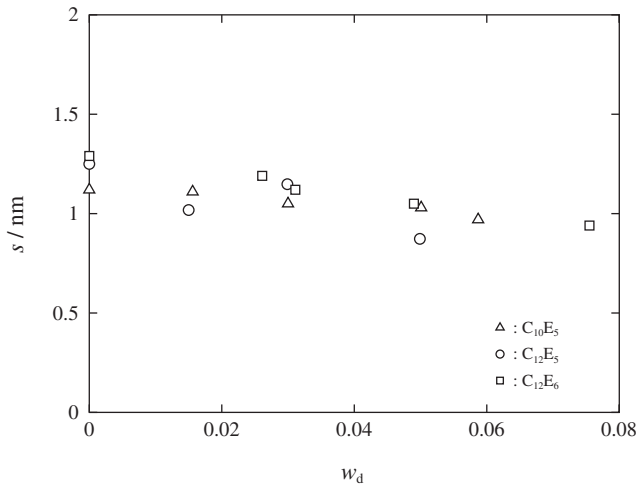

Figure 10. The spacing s of surfactant molecules on the micellar surface as a function of w_d for the $C_{10}E_5$ micelles at 20.0 °C (triangles), $C_{12}E_5$ micelles at 15.0 °C (circles), and $C_{12}E_6$ micelles at 25.0 °C (squares) containing *n*-dodecanol.

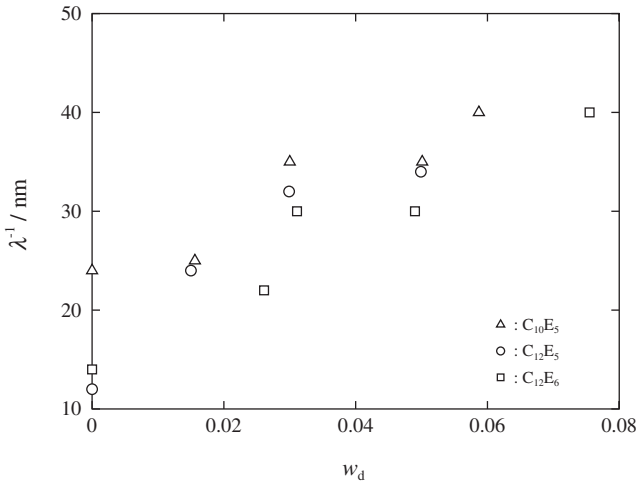

Figure 11. The stiffness parameter λ^{-1} as a function of w_d for the $C_{10}E_5$ micelles at 20.0 °C (triangles), $C_{12}E_5$ micelles at 15.0 °C (circles), and $C_{12}E_6$ micelles at 25.0 °C (squares) containing *n*-dodecanol.

gradually decreased with increasing w_d for the three micelles, implying that the surfactant molecules are more densely assembled as the *n*-dodecanol content is increased, in order to keep them inside the micelles. We find that it is substantially independent of the hydrophobic and hydrophilic chain length of the surfactant molecules.

Figure 11 illustrates w_d dependence of λ^{-1} evaluated from the analysis of the $R_{H,app}$ *vs* c plots for the $C_{12}E_5$, $C_{10}E_5$, and $C_{12}E_6$ micelles containing *n*-dodecanol. It is to be noted here the data point for the $C_{10}E_5$ micelle at $w_d = 0$ represent the result from the reanalysis of the relation between $R_{H,app}$ and c in the present work and is smaller than the previous value.[3] The λ^{-1} values for any of the three micelles increase with increasing w_d. They are roughly independent of the hydrophobic and hydrophilic chain length of the surfactant molecules with which the micelles are formed. The fact that the micelles become stiffer with uptake of *n*-dodecanol may be correlated with the result that the cross-sectional diameter of the micelles become larger as *n*-dodecanol content is increased in the micelles.

CONCLUSIONS

In the present work, we have examined variation of characteristics of the pentaoxyethylene dodecyl ether $C_{12}E_5$ micelles with uptake of *n*-dodecanol by static (SLS) and dynamic light scattering (DLS) experiments. As in the previous studies,[1–5,7–9,18] the SLS results $Kc/\Delta R_0$ successfully analyzed with the aid of the theory[10] for light scattering of micelle solutions formulated with wormlike spherocylinder model, to yield the molar mass $M_w(c)$ as a function of c along with the cross-sectional diameter d of the micelle. It has been found that the mean-square radius of gyration $\langle S^2 \rangle$ as a function of M_w is well described by the Benoit-Doty equation[12] for the wormlike chain model. The apparent hydrodynamic radius $R_{H,app}(c)$ from DLS as a function of the micellar concentration has been also successfully analyzed by the fuzzy cylinder theory by Sato *et al.*[19–21] which takes into account the hydrodynamic and direct collision interactions among micelles and allowed us to evaluate the stiffness parameter λ^{-1}. The concentration c dependence of hydrodynamic radius $R_{H,app}$ was divided into two contributions: growth of the individual "isolated" micelles with c and enhancement of hydrodynamic and direct collision interactions among micelles with c.

It has been found that the micellar length increases with increasing surfactant weight fraction w_s or with raising temperature T irrespective of the *n*-dodecanol content w_d. The length of the micelles at fixed w_s and T steeply increases with increasing weight fraction w_d of *n*-dodecanol in the $C_{12}E_5$ micelles.

The salient features on the micellar characteristics are summarized as; (i) The growth of the micelles accompanies the increase of the cross-sectional diameter d. (ii) The surfactant molecules are more densely gathered with increasing w_d in order to keep *n*-dodecanol inside the micelles. (iii) The micelles become stiffer with uptake of more *n*-dodecanol into the micelles. In comparison with previous results for the $C_{10}E_5$ and $C_{12}E_6$ micelles containing *n*-dodecanol,[18] it has been found that the values of d, s, and λ^{-1} are substantially independent of the hydrophobic and hydrophilic chain length of the surfactant molecules as far as examined in this study.

Acknowledgment. The authors are grateful to Professor T. Sato of Osaka University for valuable discussions and providing us with the computer program to calculate the apparent hydrodynamic radius.

REFERENCES AND NOTES

1. S. Yoshimura, S. Shirai, and Y. Einaga, *J. Phys. Chem. B*, **108**, 15477 (2004).
2. N. Hamada and Y. Einaga, *J. Phys. Chem. B*, **109**, 6990 (2005).
3. K. Imanishi and Y. Einaga, *J. Phys. Chem. B*, **109**, 7574 (2005).
4. Y. Einaga, A. Kusumoto, and A. Noda, *Polym. J.*, **37**, 368 (2005).
5. S. Shirai and Y. Einaga, *Polym. J.*, **37**, 913 (2005).
6. S. Shirai, S. Yoshimura, and Y. Einaga, *Polym. J.*, **38**, 37 (2006).
7. Y. Einaga, Y. Inaba, and M. Syakado, *Polym. J.*, **38**, 64 (2006).
8. Y. Einaga, Y. Kito, and M. Watanabe, *Polym. J.*, **38**, 1267 (2006).
9. K. Imanishi and Y. Einaga, *J. Phys. Chem. B*, **111**, 62 (2007).
10. T. Sato, *Langmuir*, **20**, 1095 (2004).
11. R. Koyama and T. Sato, *Macromolecules*, **35**, 2235 (2002).
12. H. Benoit and P. Doty, *J. Phys. Chem.*, **57**, 958 (1953).
13. T. Norisuye, M. Motowoka, and H. Fujita, *Macromolecules*, **12**, 320 (1979).
14. H. Yamakawa and M. Fujii, *Macromolecules*, **6**, 407 (1973).
15. H. Yamakawa and T. Yoshizaki, *Macromolecules*, **12**, 32 (1979).
16. T. Yoshizaki, I. Nitta, and H. Yamakawa, *Macromolecules*, **21**, 165 (1988).
17. Y. Einaga, Y. Totake, and H. Matsuyama, *Polym. J.*, **36**, 971 (2004).
18. M. Miyake and Y. Einaga, *J. Phys. Chem. B*, **111**, 535 (2007).
19. T. Kanematsu, T. Sato, Y. Imai, K. Ute, and T. Kitayama, *Polym. J.*, **37**, 65 (2005).
20. A. Ohshima, A. Yamagata, T. Sato, and A. Teramoto, *Macromolecules*, **32**, 8645 (1999).
21. T. Sato, A. Ohshima, and A. Teramoto, *Macromolecules*, **31**, 3094 (1998).
22. U. Menge, P. Lang, and G. H. Findenegg, *J. Phys. Chem. B*, **103**, 5768 (1999).
23. U. Menge, P. Lang, and G. H. Findenegg, *Colloids Surf., A*, **163**, 81 (2000).
24. U. Menge, P. Lang, G. H. Findenegg, and P. Strunz, *J. Phys. Chem. B*, **107**, 1316 (2003).
25. A. Bernheim-Groswasser, T. Tlusty, S. A. Safran, and Y. Talmon, *Langmuir*, **15**, 5448 (1999).
26. R. Strey, *Colloid Polym. Sci.*, **272**, 1005 (1994).
27. S. Komura, T. Takeda, Y. Kawabata, S. K. Ghosh, H. Seto, and M. Nagao, *Phys. Rev. E*, **63**, 41402 (2001).
28. T. Hellweg and D. Langevin, *Phys. Rev. E*, **57**, 6825 (1998).
29. T. Hellweg and D. Langevin, *Physica A*, **264**, 370 (1999).
30. T. Hellweg and R. von Klitzing, *Physica A*, **283**, 349 (2000).
31. S. Y. Kwon and M. W. Kim, *Langmuir*, **17**, 8016 (2001).
32. S. Y. Kwon and M. W. Kim, *Phys. Rev. Lett.*, **89**, 258302 (2002).
33. B. Berne and R. Pecora, "Dynamic Light Scattering," J. Wiley, New York, 1976.
34. H. Vink, *J. Chem. Soc., Faraday Trans. I*, **81**, 1725 (1985).
35. P. Stepanek, W. Brown, and S. Hvidt, *Macromolecules*, **29**, 8888 (1996).
36. D. Blankschtein, G. M. Thurston, and G. B. Benedek, *J. Chem. Phys.*, **85**, 7268 (1986).
37. M. E. Cates and S. J. Candau, *J. Phys.: Condens. Matter*, **2**, 6869 (1990).
38. N. Zoeller, L. Lue, and D. Blankschtein, *Langmuir*, **13**, 5258 (1997).